Carbohydrate Polymers 81 (2010) 21–28

Contents lists available at ScienceDirect

Carbohydrate Polymers

journal homepage: www.elsevier.com/locate/carbpol

On the lamellar width distributions of starch

Mateus B. Cardoso *, Harry Westfahl Jr. *

LNLS – Laboratório Nacional de Luz Síncrotron, CEP 13083-970, Caixa Postal 6192, Campinas, SP, Brazil

ARTICLE INFO

Article history:
Received 28 November 2009
Received in revised form 19 January 2010
Accepted 21 January 2010
Available online 29 January 2010

Keywords:
Starch
Lamellar organization
SAXS
Interface distribution function

ABSTRACT

Advances in the structural understanding of the lamellar organization of starch obtained through small-angle X-ray scattering (SAXS) technique are presented. An accurate starch sample preparation followed by appropriate background subtraction and Lorentz correction were able to evidence the second harmonic SAXS peak. Interface distribution functions (IDF) were generated from SAXS data to obtain dimensions and distributions of starch lamellae without any constraints or predefined assumptions. Dimensions and distributions of crystalline and amorphous lamellae were consistent with the molecular architecture of amylopectin. IDF fit results clearly indicate that amorphous and crystalline lamellae present different degrees of paracrystallinity, i.e. peak width/peak position ratios. The results of lamellar domain boundary are interpreted as a consequence of enzymatic trimming required to generate order in the amorphous lamellae for subsequent synthesis of the crystalline lattice. Amylose content seems to affect amorphous and crystalline lamellar distributions while the allomorph-type content is only reflected within the distribution of crystalline lamellae.

1. Introduction

Starch is the main reserve carbohydrate in plant tubers and endosperm seeds. Moreover, it has also been considered as a promising green hydrogen generator (Zhang, Evans, Mielenz, Hopkins, & Adams, 2007). Structurally, starch occurs as granules formed by a mixture of two distinct polysaccharide fractions, amylose and amylopectin (Buleon, Colonna, Planchot, & Ball, 1998). The amylose function on the starch micro-structure is still unclear while amylopectin is responsible for the organization of the granules into an onion-like structure of concentric soft amorphous and semi-crystalline growth rings (Gallant, Bouchet, Buleon, & Perez, 1992). The semi-crystalline growth rings are formed by alternating stacks of amorphous and crystalline lamellae (Fig. 1A), with a repetition period of ~9 nm suggesting a highly ordered biosynthetic pathway (Jenkins, Cameron, & Donald, 1993).

The crystalline lamellae of native starch are attributed to the short-chain fractions of amylopectin, the so called *A* and *B1* branches (Fig. 1B) (Tester, Karkalas, & Qi, 2004). The *A* branches corresponds to the shortest and most external amylopectin fraction, which are bounded to the slightly larger *B1* chains through $\alpha(1 \rightarrow 6)$ glucosidic bonds. These *A*–*B1* bonds enable the organization of parallel double 6-fold helices into small clusters which form either monoclinic or hexagonal unit cells (Imberty, Chanzy, Perez, Buleon, & Tran, 1988; Imberty & Perez, 1988). The clusters are packed into lamellae, separated by amorphous layers, composed by the large-chain fractions of amylopectin and the $\alpha(1 \rightarrow 6)$ glucosidic bond regions.

Small-angle X-ray scattering (SAXS) has been used to investigate the starch organization through the peak which corresponds to the lamellar periodicity of starch (Calvert, 1997). Two peak fitting models have been proposed to extract lamellar information from SAXS data of starch. The first is based on the paracrystalline fitting model where randomly oriented stacks of infinite alternating crystalline and amorphous layers are embedded in an amorphous medium (amorphous growth rings) (Cameron & Donald, 1992). The second one, called side-chain liquid crystalline polymers model, considers starch as a finite stack of alternating lamellae that are allowed to thermally fluctuate both along the layer repeat direction and the transverse layer direction (Daniels & Donald, 2003). In both models, crystalline and amorphous lamellae are assumed to follow Gaussian distributions with the same degree of paracrystallinity, i.e. peak width/peak position ratio. In spite of the success of these models to qualitatively describe several structural and thermodynamic aspects of starch, the physical meaning of the layer width distribution is hindered through this simplification.

In general, SAXS curves of semi-crystalline polymers can be either directly fitted through a mathematical model or Fourier transformed into the interface distribution function (IDF) (Stribeck, 2007). Though the former method is a direct fit approach, it is more susceptible to numerical instabilities of the least-square procedures while the latter has shown to be more stable and with faster numerical convergence. IDFs are obtained through the Fourier

* Corresponding authors. Tel.: +55 19 3512 1045; fax: +55 19 3512 1004 (M.B. Cardoso); tel.: +55 19 3512 1034 (H. Westfahl Jr.).
E-mail addresses: cardosomb@lnls.br (M.B. Cardoso), westfahl@lnls.br (H. Westfahl Jr.).

0144-8617/$ - see front matter © 2010 Elsevier Ltd. All rights reserved.
doi:10.1016/j.carbpol.2010.01.049

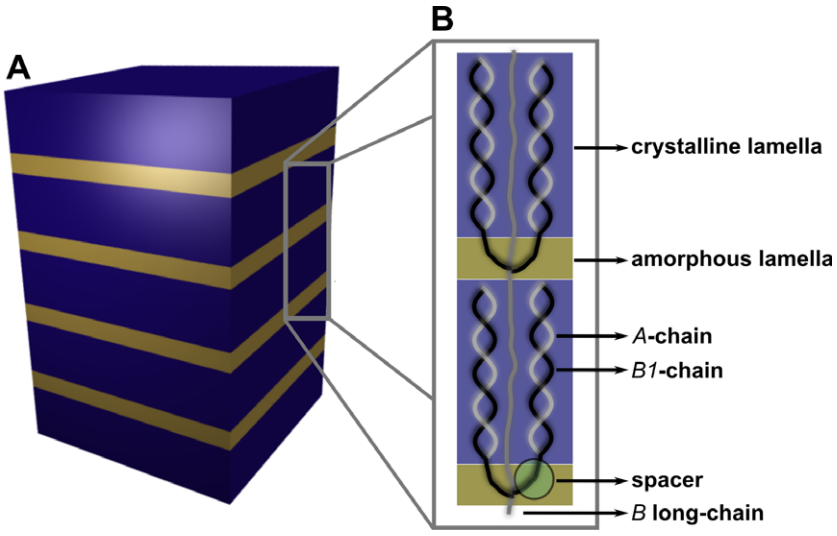

Fig. 1. Schematic drawing of the lamellar organization of starch. (A) Representation of the lamellar stacks of starch. (B) Amorphous and crystalline lamellar representation evidencing different parts of the amylopectine architecture.

transform of the data after the extraction of background density fluctuations and the application of Porod-law (Hsiao & Verma, 1998; Stribeck & Ruland, 1978). Through IDF fits a full characterization of the polymer lamellae is achieved and the width distributions for crystalline and amorphous lamellar phases are obtained.

In this work, we focused our efforts on the structural understanding of starch lamellar organization through the analysis of SAXS data. Starch SAXS data were obtained and contributions from background density fluctuations and finite interface between the phases were subtracted following a procedure similar to the one proposed by Hsiao and Verma (1998). Lorentz corrected SAXS data were then Fourier transformed to obtain IDF functions of starch samples. Gaussian distributions were computed to fit IDF patterns to represent the variation of interface distances of starch lamellae using the approach proposed by Stribeck and Ruland (1978). Although both procedures are well know and widely applied into the semi-crystalline polymers characterization, they have never been explored within the context of starch ultrastructure.

2. Materials and methods

2.1. Materials

Normal maize starch was purchased from Aldrich and waxy maize starch was a kind gift of Prof. Antônio Aprigio da Silva Curvelo. Both maize starches were used as received. Pinhão starch was obtained from seeds of *Araucaria angustifolia* and isolated through successive washes with water (Thys et al., 2008). The efficiency of starch isolation was verified using fluorescence spectroscopy (Cardoso, Putaux, Samios, & da Silveira, 2007; Cardoso, Samios, & Silveira, 2006). The amylose content was determined by means of enzymatic method (kit K-AMYL 04/06, Megazyme International Ireland Ltd., Ireland). Milli-Q water was used in all experimental procedures.

2.2. Scanning electron microscopy (SEM)

Micrographs were recorded using a JEOL JSM 6060 microscope (JEOL, Tokyo, Japan) at the Brazilian Synchrotron Light Laboratory (LNLS). Drops of granule suspensions were allowed to dry onto copper stubs and the specimens were coated with gold. SEM observations were performed in secondary electron mode operating at 8.0 kV.

2.3. Wide-angle X-ray diffraction (WAXD)

WAXD diagrams were recorded on the D03B beamline using a fixed radiation wavelength (λ = 1.425 Å) at the Brazilian Synchrotron Light Laboratory (LNLS). Diffraction patterns were recorded during 1 min exposures on a marCCD 165 detector (4 × 4 binning) placed 100.0 mm away from the sample. Calibration was achieved using an alumina pattern. Measurements were made on samples after water content adjustment by sorption at 90% relative humidity (RH) for 9 days in the presence of a saturated sodium chloride solution under partial vacuum. The samples were prepared in thin-walled (0.01 mm) glass capillary tubes (1.0 mm in diameter). The capillaries were centrifuged to pack the granules at the bottom and sealed in order to prevent any significant change in water content during the measurements. WAXD profiles were obtained by radial averaging and normalized to the integrated area covering a scattering vector q ($q = (4\pi/\lambda)\ \sin\theta$; 2θ = scattering angle) ranging from 2.4 to 28.0 nm^{-1}. The WAXD patterns were used to determine the crystallinity and respective amount of A- and B-type allomorphs as described in the literature (Thys et al., 2008).

2.4. Small-angle X-ray scattering (SAXS)

SAXS measurements were performed on the D2A beamline at the Brazilian Synchrotron Light Laboratory (LNLS). The incident X-ray monochromatic beam (λ = 1.488 Å) was monitored with a photomultiplier and detected on a marCCD 165 detector (8 × 8 binning). The sample-to-detector distance was 1088 mm long, covering a scattering vector q ranging from 0.1 to 2.7 nm^{-1}.

Dried starch samples were weighted (15.0 ± 0.3 mg) and placed between two mica sheets. Water was carefully added (15 μL) to starch and the sample holder was sealed to prevent any change in water amount during experiments. The collimated X-ray beam was passed horizontally through a chamber containing the sample. The measurements were performed at room temperature and each SAXS pattern was cumulated for 1 min. No evidence of starch degradation was observed for exposures up to 1.5 min. Silver behenate powder was used as standard to calibrate the sample-to-detector distance, the detector tilt and the direct beam position. Transmission, dark current and mica sheet corrections were performed on the 2D image before further data processing. The isotropic scattering patterns were radially averaged.

In order to analyze the SAXS data, contributions from background density fluctuations and finite interface between the phases were first removed (Hsiao & Verma, 1998; Stribeck, 2007) and the remaining scattered intensities were Lorentz corrected (Glatter & Kratky, 1982; Stribeck, 2007). Interface distribution functions (IDF) were obtained from the second derivative of the Fourier transformed scattering intensity (Ruland, 1977; Stribeck & Ruland, 1978). IDF fits were computed by modeling Gaussian distributions to represent the variation of interface distances (Stribeck & Ruland, 1978). The quality of the fit to the data was evaluated using the Levenberg–Marquardt minimization of the χ^2 parameter merit function (least-squares). This method is implemented in the NonlinearRegress procedure of Mathematica 6.0 from Wolfram Research (Henkelman, 2008). Further information about data evaluation and IDF processing are given in Appendix A.

3. Results

3.1. Preliminary starch characterization

Fig. 2 presents SEM images and granule size distributions for normal maize, pinhão and waxy maize starches.

As observed previously, normal maize starches coexist into a variety of granule shapes such as spherical and polyhedral (Fig. 2A) (Glaring, Koch, & Blennow, 2006; Kuakpetoon & Wang, 2008; Kuo & Lai, 2007; Zhang, Ao, & Hamaker, 2006). In general, it is observed that spherical maize granules tend to be smaller in size when compared to the polyhedral ones (Bello-Perez et al., 2006; Kuo & Lai, 2007; Zhang et al., 2006). It is reflected in a bimodal distribution which clearly shows the difference in size between the shapes (Fig. 2B). The first starch population, which is mainly attributed to spherical maize granules, is centered at 4.8 μm presenting a polydispersity index of 77.8% (Table 1). The second population is basically formed by polyhedral starch granules. This larger distribution presents the mean granule size of 11.7 μm and a polydispersity index of 56.2%.

Fig. 2C shows a representative SEM image of pinhão starches where a variety of shapes is also seen. Although pinhão starch granules present a coexistence of oval and truncated ellipsoid granules, a monomodal size distribution is observed. The granules size typically ranges from 6 to 21 μm while exhibits a distribution centered at 12.5 μm (Fig. 2D) (Bello-Perez et al., 2006; Thys et al., 2008). The polydispersity index of pinhão starch distribution (20.8%) is significantly smaller than those obtained for normal maize starch indicating a regulated granule size synthesis. Waxy maize granules are also observed through a mixture of different shapes. Similarly to normal maize starch, polyhedral and spherical granules are observed (Fig. 2E). However, a monomodal distribution was obtained with sizes ranging from 3 to 19 μm (Franco, Ciacco, & Tavares, 1998). The waxy starch distribution is centered at 10.1 μm presenting a polydispersity index of 62.9% (Fig. 2F).

Complementary to SEM images and granule size distributions, total amylose contents for normal maize, pinhão and waxy maize starches are also presented in Table 1.

Normal maize and pinhão starches present 27.2% and 25.7% of amylose in their composition, respectively. On the other hand, waxy maize granules had around 1.0% of total amylose content. As expected, a significant difference is observed in the total amylose content due to the reduced amount of amylose present in waxy starch granules (Liu, Yu, Simon, Dean, & Chen, 2009; Putaux, Molina-Boisseau, Momaur, & Dufresne, 2003).

Fig. 3 shows the WAXD patterns and their respective diffraction peak fittings for normal maize, pinhão and waxy maize starches.

Normal and waxy maize starches present the typical A-type allomorph profile mainly characterized through the peaks at around 10.8, 12.8 and 16.4 nm^{-1} (Fig. 3A and C). The crystallinity index (CI) obtained by means of the peaks fitting indicates 30.9% and 31.5% of crystalline material into normal and waxy maize starches, respectively (Table 1). The typical C-type profile, with peaks characteristic of A- and B-type allomorphs (main B-type allo-

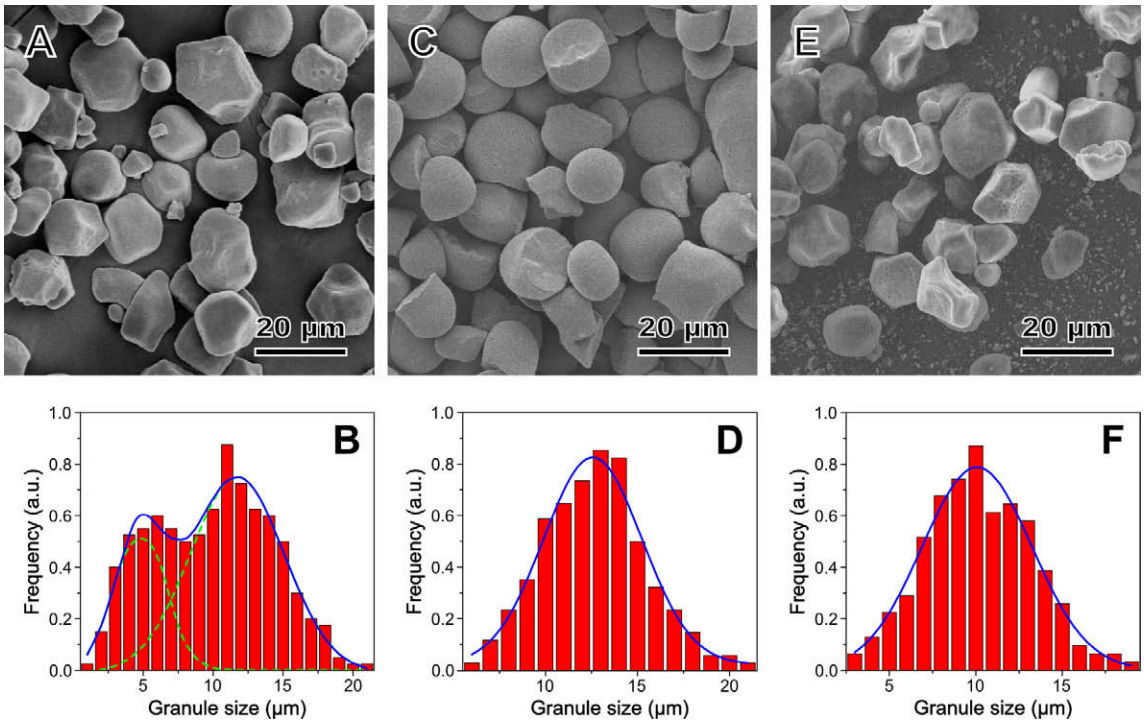

Fig. 2. Scanning electron microscopy images and their respective granule size distributions. (A and B) Normal maize starch; (C and D) pinhão starch; (E and F) waxy maize starch.

Table 1
Average granule size, polydispersity, amylose content, allomorph profile, crystallinity index and structural parameters obtained from the evaluation of interface distribution functions and Porod-law for normal maize, pinhão, and waxy maize starches.

Sample		Average granule size (μm)	Polydispersity (%)	Amylose content (%)	Allomorph profile	Crystallinity index (%)	d_c (nm)	σ_c (nm)	d_a (nm)	σ_a (nm)	L (nm)	t (nm)	d_z (nm)
Normal maize	1st population	4.8	77.8	27.2	A-type	30.0	6.4 ± 0.1	2.3 ± 0.1	2.2 ± 0.2	1.0 ± 0.2	8.6	–	0.19
	2nd population	11.7	56.2										
Pinhão		12.5	20.8	25.7	C-type	32.2	6.8 ± 0.1	2.1 ± 0.2	1.9 ± 0.1	0.9 ± 0.2	8.7	470	0.20
Waxy maize		10.1	62.9	~1.0	A-type	31.5	5.9 ± 0.2	1.8 ± 0.2	2.4 ± 0.1	1.5 ± 0.1	8.3	–	0.19

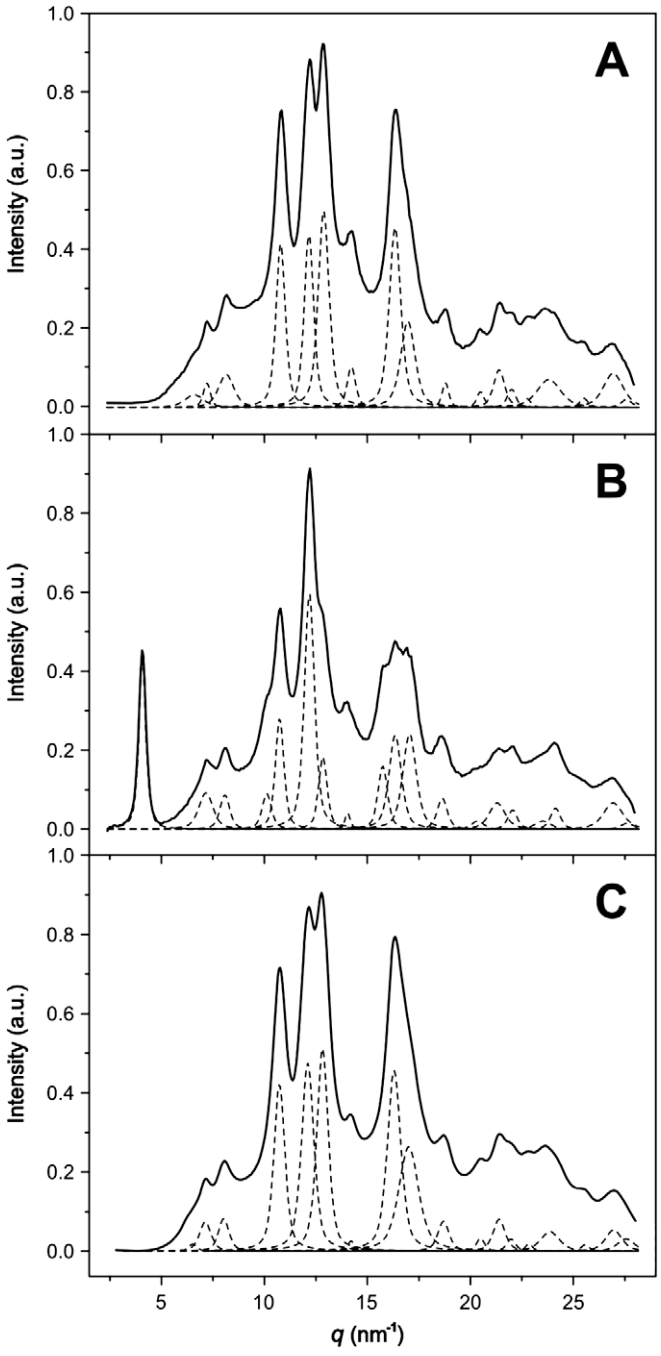

Fig. 3. Wide-angle X-ray diffraction starch diagrams (solid lines) and their respective crystalline peak fits (dashed lines) for (A) normal maize; (B) pinhão; and (C) waxy maize starches.

morph peaks are located at 4.1, 15.8 and 17.0 nm^{-1}), can be seen in the WAXD diagram of pinhão starch (Fig. 3B). This WAXD profile suggests that pinhão starch is composed by a mixture of A- and B-type crystallites. Pinhão starch presented $CI = 32.2\%$ while the relative proportions of A- and B-type allomorphs were 46% and 54%, respectively.

3.2. SAXS analysis

Fig. 4 presents experimental SAXS data (open circles) for (A) normal maize, (B) pinhão and (C) waxy maize starches after background subtraction and Lorentz correction. Solid red line starting at $q \sim 2.3\ nm^{-1}$ represents the Porod-law applied to extrapolate the experimental SAXS data to $q \to \infty$.

Although all starch samples have an almost identical main SAXS peak, subtle differences are observed when the maximum peak positions are compared. Normal maize, pinhão and waxy maize starches present the main peak position located at $q = 0.64$, 0.65 and 0.67 nm^{-1}, respectively. These values are in agreement with those published earlier (Calvert, 1997; Cameron & Donald, 1992; Jenkins et al., 1993; Vermeylen, Goderis, Reynaers, & Delcour, 2004). Surprisingly, the second starch reflection peak, indicated by the arrows in Fig. 4, is for the first time observed ($q \sim 1.3\ nm^{-1}$). The appearing of this unexpected second reflection order is attributed to an accurate background subtraction as well as a good signal-to-noise ratio obtained during SAXS experiments. Although the patterns of the second reflection peaks highly resemble between the different starch species studied here, waxy maize granules presented a less intense and slightly shifted peak ($q \sim 1.4\ nm^{-1}$) if compared to normal maize and pinhão starches.

IDFs (open circles in Fig. 5, left panel) were obtained by applying the second derivative to the Fourier transformed SAXS data. For all samples, the periodicity of the lamellar system is pronounced since IDF peaks until 4th order can be observed.

IDF fits (solid red lines in Fig. 5, left panel) were computed assuming independent Gaussian distributions for amorphous and crystalline lamellae (details about IDFs and the structure parameters determined in the data fits are given in Appendix A). The quality of the fits was evaluated by means of ANOVA table (Miller, 1997) results and a good agreement between IDFs and their fits is observed. The degree of correlation of IDF fits for normal maize, pinhão and waxy maize starches are 0.99, 0.99 and 0.98, respectively. The right panel of Fig. 5 shows the layer-thickness distributions resulting from the IDF fits. Dotted orange line distributions represent the amorphous lamellae which exhibit symmetric and relatively narrow size distributions. The broad dashed blue line distributions correspond to the crystalline lamellar regions and the overall lamellar repetitions are the solid green line curves pointing towards negative values, as expected for IDFs. In spite of the differences on the average thickness of amorphous lamellae (d_a) and long periods (L), the average thickness of crystalline lamellae (d_c) is in agreement with results obtained through direct peak

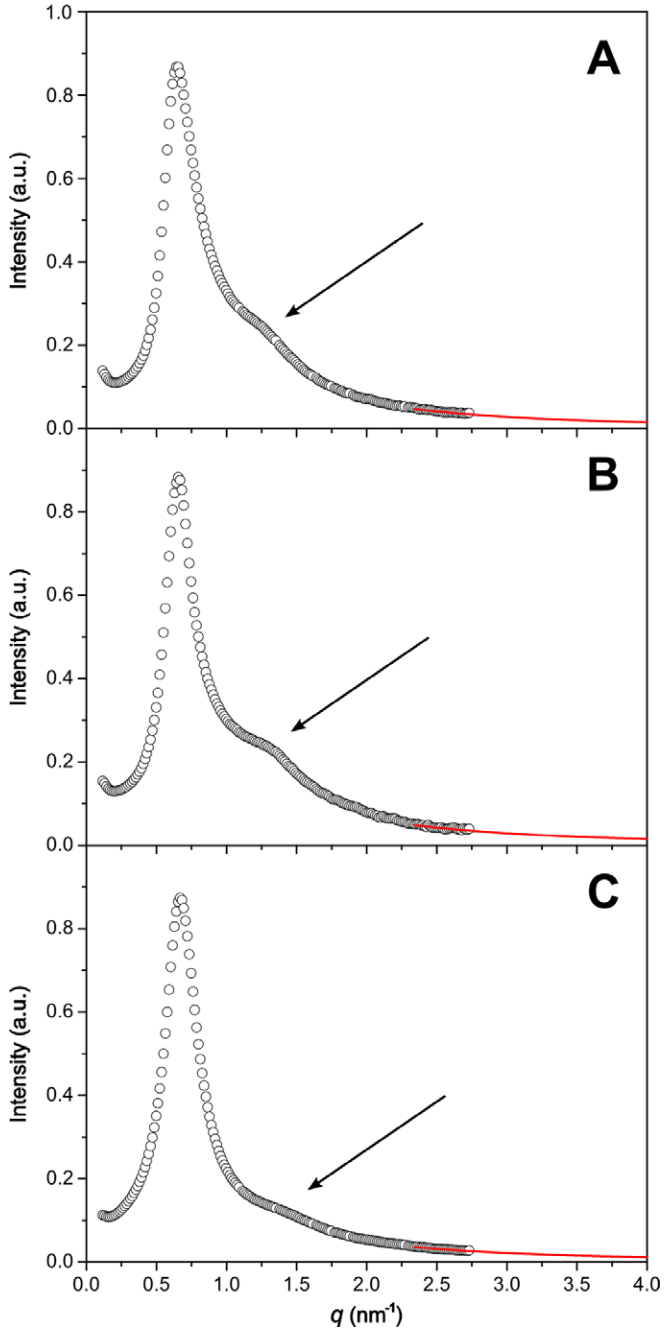

Fig. 4. Lorentz corrected and background subtracted SAXS data (open circles) and their respective Porod extrapolations (solid red lines). (A) Normal maize starch; (B) pinhão starch; and (C) waxy maize starch. The arrows indicate the presence of second ordering starch peak.

fittings (Cameron & Donald, 1992; Daniels & Donald, 2003; Thys et al., 2008). The predicted pitch size for a 6-fold helix is ~2 nm (Imberty & Perez, 1988; Imberty et al., 1988). Thus, d_c values between 5.9 and 6.8 nm correspond to ~3 helical pitches per crystalline lamella. The standard deviation of the crystalline lamellae (σ_c) is ~2 nm which represents ~1 helical pitch. This is reasonable since it is expected that double-helices containing less than 2 pitches are energetically unstable (Gidley & Bulpin, 1987). On the other hand, the inexistence of helices with more than 4 pitches can be explained due to the low probability of finding *A* chains having more than 24 glucose residues (Tester et al., 2004). The average size of amorphous lamellae ($d_a \sim 2.2$ nm) is significantly smaller than those obtained through direct peak fittings ($d_a \sim 2.8$ nm) (Cameron & Donald, 1992; Daniels & Donald, 2003). These lamellae are formed by large-chain fractions of amylopectin and by the length difference between *A* and *B1* chains (the so called spacer chains – Fig. 1) (Waigh, Perry, Riekel, Gidley, & Donald, 1998), which is usually ~8 glucose monomers for most common botanical species (Gidley & Bulpin, 1987; Hizukuri, 1986). Moreover, the spacer chains are also closely attached to the amorphous-crystalline interface through $\alpha(1 \rightarrow 6)$ glucosidic bonds, resulting in a steric tendency to be aligned on the radial direction, within a length scale of order of 2 nm. The width (σ_a) of amorphous layer distributions is relatively larger reaching ~50% of d_a values. This probably reflects the variety of configurations and the length distribution of spacer chains, since we suppose that the influence of large-chain fractions of amylopectin has a minor importance in the lamellar amorphous dimension. Long period, *L*, obtained from the IDF analysis are between 8.3 and 8.7 nm, which are slightly smaller than the results of the direct peak fitting which are usually around 9.0 nm (Cameron & Donald, 1992; Daniels & Donald, 2003; Thys et al., 2008). This reduction was already predicted, because a fit on the scattering intensity systematically overestimates the bigger long periods (Stribeck, 2007). The decrease of *L* is interpreted as a consequence of d_a reduction. Further, it is important to mention here that the lamellar distributions obtained by IDF did not present the same peak width/peak position ratio as suggested through direct peak fittings (Cameron & Donald, 1992; Daniels & Donald, 2003).

The correlation range, *t*, (details in Appendix A) corresponds to the average number of correlated lamellar periods and is related to the average thickness of the semi-crystalline growth rings. The *t* value for pinhão starch is 470 nm and indicates a correlation length of ~50 lamellar period repetitions. This value is lightly larger than those obtained through direct peak fitting (Hsiao & Verma, 1998). However, it is important to note that direct peak fitting has not shown to be sensitive to variations in the overall lamellar repetition parameter (Daniels & Donald, 2003; Stribeck & Ruland, 1978). *t* value obtained for normal and waxy maize starches are infinity which indicates that the limited low-*q* range of our experimental setup hinders proper *t* value calculation.

The thickness of the domain boundary zone, d_z, (details in Appendix A) was determined from the deviation of the measured Porod-law from the ideal one. The results obtained (Table 1) are smaller than those previously determined for rice and potato starches (Vermeylen et al., 2006) and may be an artefact of the extrapolation procedure adopted here. Nevertheless, we interpret these results as a consequence of enzymatic trimming (Ball et al., 1996; Mouille et al., 1996) required to generate order in the amorphous lamella for subsequent synthesis of the crystalline lattice, as illustrated in Fig. 6.

The schematic drawing shows the initial step of the crystalline lamellar synthesis where helices with different lengths are formed (Fig. 6A). According to the trimming model, enzymes are responsible for removing the gray glycosidic region which is located above the lamellar plane shown as blue double-helices. In this mechanism, the enzymes act in order to minimize the difference in length of the double-helices which generate a smooth surface as shown in Fig. 6B. In this way, the small values of d_z are interpreted as consequence of the enzymatic effect which allows to a significant sharp domain boundary.

4. Discussion

Although several works have been discussing an efficient way of describing the lamellar organization of starch, the focus on the first and well described SAXS ordering peak ($q \sim 0.6$ nm^{-1}) as well as the lack of knowledge about the second ordering reflection ($q \sim 1.3$ nm^{-1}) may have allowed a difficult interpretation of the

nature of the lamellar starch organization. In this work, an important advance on the lamellar starch organization is yielded since the second ordering peak is observed as a result of a careful processing of SAXS data. This surprisingly finding changed the most general view on starch SAXS patterns where a single and broad peak was interpreted as the unique evidence due to the lamellar organization of the granules (Cameron & Donald, 1992; Daniels & Donald, 2003; Thys et al., 2008; Vermeylen et al., 2004). This 'new' starch SAXS pattern containing two broad peaks is highly similar to those of semi-crystalline polymers where the paracrystalline lamellar order is observed (Choi, Vaidya, Han, Sota, & Hashimoto, 2003; Hama & Tashiro, 2003; Ivanov, Bar, Dosiere, & Koch, 2008; Bliznyuk et al., 2008). Thus, we interpret the evidence of second ordering peak of starch as well as the similarity between SAXS patterns of starch and semi-crystalline polymers as a confirmation of the paracrystalline nature of starch lamellae.

Direct fitting approaches have used Gaussian functions in order to describe crystalline and amorphous lamellar distributions of starch. Therefore, all these approaches have arbitrarily assumed that amorphous and crystalline distributions present identical degree of paracrystallinity, i.e. peak width/peak position ratio (σ/d). Even considering that a qualitative description of starch lamellae has been successfully achieved through these methods, the physical meaning of the lamellar distribution is lost since this constraint

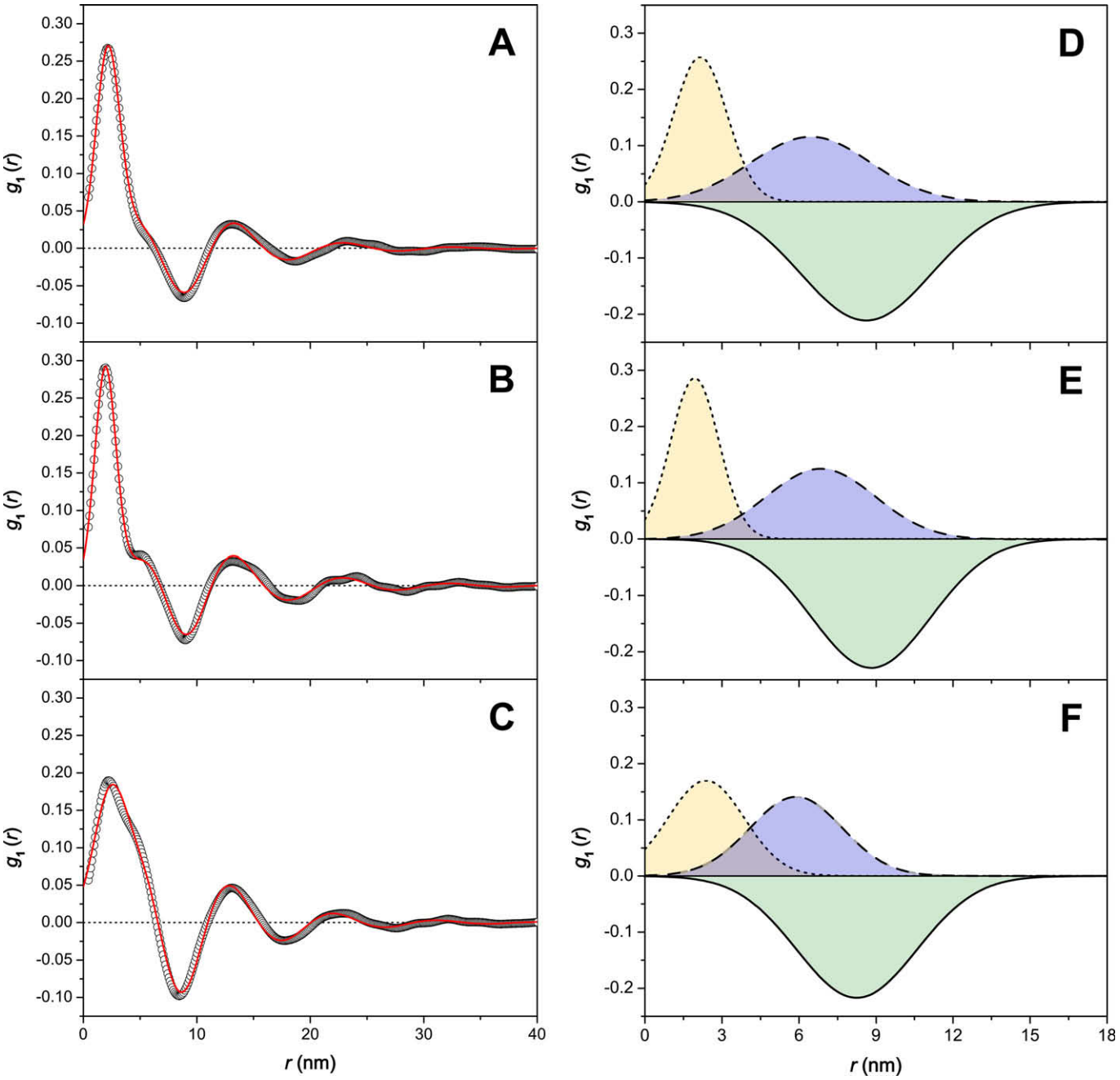

Fig. 5. Left Panel: Interface distribution function (open circles) and their corresponding fits (solid red lines) for (A) normal maize, (B) pinhão; and (C) waxy maize starches. Right panel: Separated lamellae layer-thickness distributions as resulting from the IDF fit presented in left panel. Dotted orange lines: amorphous layer thicknesses. Dashed blue lines: crystalline layer thicknesses. Solid green lines: twin-layer thicknesses (i.e. amorphous + crystalline = long periods). (D) Normal maize starch; (E) pinhão starch; (F) waxy maize starch. (For interpretation of the references to color in this figure legend, the reader is referred to the web version of this paper.)

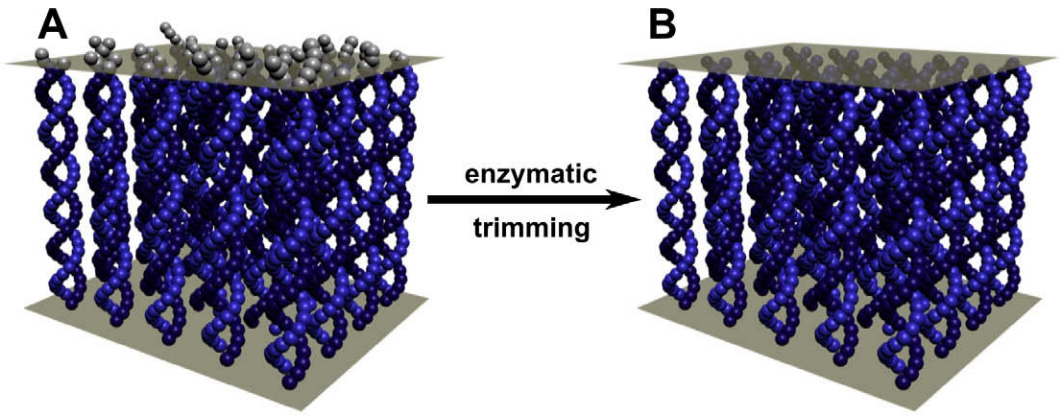

Fig. 6. Schematic drawing of the enzymatic trimming effect during lamellar starch synthesis. Double-helices represent the crystalline lamella (A) before and (B) after enzymatic trimming. Planes perpendicular to the helices were inserted only for visualization purpose.

implies identical degrees of paracrystallinity for amorphous and crystalline layers. In contrast, in this work, we report the first IDF analysis applied to starch where lamellar dimensions and distributions are obtained without any assumption.

In spite of the degree of similarity between starch SAXS profiles, IDFs and their fits, we have shown that significant differences and similarities can be pointed out when lamellar distributions are compared. Although normal maize and pinhão starches presented different granule size and crystalline type, similar IDF profiles were observed (Fig. 5). Narrow and relatively intense lamellar amorphous distributions, presenting almost the same values of d_a and σ_a, were seen for both starch species (Table 1). On the other hand, normal maize and pinhão starches present subtle differences of d_c values. In this case, we speculate that these differences are mainly related to the crystalline-type profile of each botanical starch specie. Normal maize is described as a typical A-type starch allomorph while pinhão shows the C-type pattern (Fig. 3) which represents the coexistence of A- and B-type crystallites within the same granule. However, B-type allomorphs tend to have longer amylopectin branch chain lengths which would allow increasing the average size of the crystalline lamellae (Hizukuri, 1986). Thus, we suggest that the B-type crystallites found in pinhão starches are the main responsible for this increase of d_c values.

In parallel, normal and waxy maize starches can be compared taking into account the amylose content of the granules since they have the same crystalline-type profile and similar size. Distinct IDF profiles are observed (Fig. 5A and C) which reflect structural differences in the lamellar distribution of starches (Fig. 5D and F). Waxy maize starch presented larger mean size, broader and less intense amorphous lamellar distribution than normal maize starch. On the other hand, smaller average dimension and sharper crystalline lamellar distribution was obtained for waxy starch. It probably indicates that the amylose content plays distinct roles in the amorphous and crystalline lamellar organization. While in amorphous lamella the presence of amylose decrease its size and polydispersity, a significant increase of the crystalline lamella size is observed when the amylose content of the granule is increased.

Although it is difficult to statistically compare the degree of success of different modeling procedures, IDF allowed obtaining the real degree of paracrystallinity of the lamellae which represents a significant advance in the structural characterization of starch. In IDF method σ/d for the amorphous fraction is ~0.5. Admittedly, Fig. 5D–F show that the corresponding leftmost peak extends somewhat into the negative range. Thus, the fit artificially widens the distribution of the amorphous layers in order to compensate the surface roughness effect of the crystallites to the IDF. Nevertheless, this artificial widening is not significant in order to explain the discrepancy in the values found by direct fitting procedures (values generally between 0.2 and 0.3). We suppose that these small values of σ_a/d_a obtained in direct fitting methods are related to the constraint applied, $\sigma_a/d_a = \sigma_c/d_c$. It allows an overestimation of the size of amorphous lamellae, since in direct fitting approaches the average size of d_a is ~2.8 nm while in IDF method is ~2.2 nm. On the other hand, independent of the modeling procedure, only subtle differences were seen when crystalline lamellar dimensions (d_c or σ_c/d_c) were taken into account. Moreover, we consider that the values of σ_a and σ_c obtained in this work are realistic since they are well correlated with the molecular architecture of amylopectin. σ_a is related to the diversity of possible configurations and sizes of the spacer chains while σ_c is interpreted as the variation in size of stable starch helices (Bertoft, 2007). This clear correlation between different values of σ_a and σ_c and the structure of amylopectin allows believing that IDF method was able to obtain more reliable results than the previous models found in the literature (Cameron & Donald, 1992; Daniels & Donald, 2003).

5. Conclusions

In summary, we have demonstrated that a thorough analysis of carefully processed starch SAXS data leads to evidence of second harmonic peak. IDFs obtained from Lorentz corrected SAXS data were fitted to obtain lamellar distributions of starch. The average size of the crystalline region corresponds to lamellae which are formed by double-helices of approximately 3 pitches while the size of the amorphous region is mainly related to the difference in chain length between *A* and *B1* short segments of amylopectin. Gaussian lamellar distributions show that the degree of paracrystallinity of the amorphous region tends to be relatively larger than the crystalline. The ordering generated during the lamellae synthesis proposed by the enzymatic trimming model is reflected in the sharp domain boundary results. Considerable changes within the lamellar structure of starch seem to be much more related to the amylose content than to the crystalline-type structure. IDF showed to be a fitting approach which is able to discriminate significant lamellar differences between starches of distinct botanical origins.

Acknowledgments

LNLS is acknowledged through the projects D11A-6692 (SAXS), MX1-6948 (WAXD) and LV-6897 (SEM). We thank Sai V. Pingali and Hugh O'Neill for critical reading of this paper. Fernando Carlos Giacomelli is acknowledged for his support with WAXD experiments. We specially thank Antônio José Ramirez and Paulo Silva (LME–LNLS) for SEM analysis.

Appendix A. Supplementary data

Supplementary data associated with this article can be found, in the online version, at doi:10.1016/j.carbpol.2010.01.049.

References

Ball, S., Guan, H. P., James, M., Myers, A., Keeling, P., Mouille, G., et al. (1996). From glycogen to amylopectin: A model for the biogenesis of the plant starch granule. *Cell, 86*(3), 349–352.

Bello-Perez, L. A., Garcia-Suarez, F. J., Mendez-Montealvo, G., do Nascimento, J. R. O., Lajolo, F. M., & Cordenunsi, B. R. (2006). Isolation and characterization of starch from seeds of *Araucaria brasiliensis*: A novel starch for application in food industry. *Starch-Starke, 58*(6), 283–291.

Bertoft, E. (2007). Composition of building blocks in clusters from potato amylopectin. *Carbohydrate Polymers, 70*(1), 123–136.

Bliznyuk, V. N., Tereshchenko, T. A., Gumenna, M. A., Gomza, Y. P., Shevchuk, A. V., Klimenko, N. S., et al. (2008). Structure of segmented poly(ether urethane)s containing amino and hydroxyl functionalized polyhedral oligomeric silsesquioxanes (POSS). *Polymer, 49*(9), 2298–2305.

Buleon, A., Colonna, P., Planchot, V., & Ball, S. (1998). Starch granules: Structure and biosynthesis. *International Journal of Biological Macromolecules, 23*(2), 85–112.

Calvert, P. (1997). Biopolymers – the structure of starch. *Nature, 389*(6649), 338–339.

Cameron, R. E., & Donald, A. M. (1992). A small-angle X-ray-scattering study of the annealing and gelatinization of starch. *Polymer, 33*(12), 2628–2636.

Cardoso, M. B., Putaux, J. L., Samios, D., & da Silveira, N. P. (2007). Influence of alkali concentration on the deproteinization and/or gelatinization of rice starch. *Carbohydrate Polymers, 70*, 160–165.

Cardoso, M. B., Samios, D., & Silveira, N. P. (2006). Study of protein detection and ultrastructure of Brazilian rice starch during alkaline extraction. *Starch-Starke, 58*(7), 345–352.

Choi, S. B., Vaidya, N. Y., Han, C. D., Sota, N., & Hashimoto, T. (2003). Effects of sample preparation method and thermal history on phase transition in highly asymmetric block copolymer: Comparison with symmetric block copolymers. *Macromolecules, 36*(20), 7707–7720.

Daniels, D. R., & Donald, A. M. (2003). An improved model for analyzing the small angle X-ray scattering of starch granules. *Biopolymers, 69*(2), 165–175.

Franco, C. M. L., Ciacco, C. F., & Tavares, D. Q. (1998). The structure of waxy corn starch: Effect of granule size. *Starch-Starke, 50*(5), 193–198.

Gallant, D. J., Bouchet, B., Buleon, A., & Perez, S. (1992). Physical characteristics of starch granules and susceptibility to enzymatic degradation. *European Journal of Clinical Nutrition, 46*, S3–S16.

Gidley, M. J., & Bulpin, P. V. (1987). Crystallization of maltooligosaccharides as models of the crystalline forms of starch - minimum chain-length requirement for the formation of double helice. *Carbohydrate Research, 161*(2), 291–300.

Glaring, M. A., Koch, C. B., & Blennow, A. (2006). Genotype-specific spatial distribution of starch molecules in the starch granule: A combined CLSM and SEM approach. *Biomacromolecules, 7*(8), 2310–2320.

Glatter, O., & Kratky, O. (1982). *Small angle X-ray scattering*. Academic Press Inc..

Hama, H., & Tashiro, K. (2003). Structural changes in isothermal crystallization process of polyoxymethylene investigated by time-resolved FTIR, SAXS and WAXS measurements. *Polymer, 44*(22), 6973–6988.

Henkelman, G. (2008). Mathematica 6.0. *Journal of the American Chemical Society, 130*(2), 775.

Hizukuri, S. (1986). Polymodal distribution of the chain lengths of amylopectins, and its significance. *Carbohydrate Research, 147*(2), 342–347.

Hsiao, B. S., & Verma, R. K. (1998). A novel approach to extract morphological variables in crystalline polymers from time-resolved synchrotron SAXS data. *Journal of Synchrotron Radiation, 5*, 23–29.

Imberty, A., Chanzy, H., Perez, S., Buleon, A., & Tran, V. (1988). The double-helical nature of the crystalline part of A-starch. *Journal of Molecular Biology, 201*(2), 365–378.

Imberty, A., & Perez, S. (1988). A revisit to the 3-dimensional structure of B-type starch. *Biopolymers, 27*(8), 1205–1221.

Ivanov, D. A., Bar, G., Dosiere, M., & Koch, M. H. J. (2008). A novel view on crystallization and melting of semirigid chain polymers: The case of poly (trimethylene terephthalate). *Macromolecules, 41*(23), 9224–9233.

Jenkins, J. P. J., Cameron, R. E., & Donald, A. M. (1993). A universal feature in the structure of starch granules from different botanical sources. *Starch-Starke, 45*(12), 417–420.

Kuakpetoon, D., & Wang, Y. J. (2008). Locations of hypochlorite oxidation in corn starches varying in amylose content. *Carbohydrate Research, 343*(1), 90–100.

Kuo, W. Y., & Lai, H. M. (2007). Changes of property and morphology of cationic corn starches. *Carbohydrate Polymers, 69*(3), 544–553.

Liu, H. S., Yu, L., Simon, G., Dean, K., & Chen, L. (2009). Effects of annealing on gelatinization and microstructures of corn starches with different amylose/amylopectin ratios. *Carbohydrate Polymers, 77*(3), 662–669.

Miller, R. G. (1997). *Beyond ANOVA: Basics of Applied Statistics*. Chapman & Hall.

Mouille, G., Maddelein, M. L., Libessart, N., Talaga, P., Decq, A., Delrue, B., et al. (1996). Preamylopectin processing: A mandatory step for starch biosynthesis in plants. *Plant Cell, 8*(8), 1353–1366.

Putaux, J. L., Molina-Boisseau, S., Momaur, T., & Dufresne, A. (2003). Platelet nanocrystals resulting from the disruption of waxy maize starch granules by acid hydrolysis. *Biomacromolecules, 4*(5), 1198–1202.

Ruland, W. (1977). Density fluctuations in amorphous and semicrystalline polymers. *Pure and Applied Chemistry, 49*(7), 905–913.

Stribeck, N. (2007). *X-Ray Scattering of Soft Matter*. Springer Laboratory.

Stribeck, N., & Ruland, W. (1978). Determination of interface distribution function of lamellar 2-phase systems. *Journal of Applied Crystallography, 11*, 535–539.

Tester, R. F., Karkalas, J., & Qi, X. (2004). Starch-composition, fine structure and architecture. *Journal of Cereal Science, 39*(2), 151–165.

Thys, R. C. S., Westfahl, H., Norena, C. P. Z., Marczak, L. D. F., Silveira, N. P., & Cardoso, M. B. (2008). Effect of the alkaline treatment on the ultrastructure of C-type starch granules. *Biomacromolecules, 9*(7), 1894–1901.

Vermeylen, R., Derycke, V., Delcour, J. A., Goderis, B., Reynaers, H., & Koch, M. H. J. (2006). Gelatinization of starch in excess water: Beyond the melting of lamellar crystallites. A combined wide- and small-angle X-ray scattering study. *Biomacromolecules, 7*(9), 2624–2630.

Vermeylen, R., Goderis, B., Reynaers, H., & Delcour, J. A. (2004). Amylopectin molecular structure reflected in macromolecular organization of granular starch. *Biomacromolecules, 5*(5), 1775–1786.

Waigh, T. A., Perry, P., Riekel, C., Gidley, M. J., & Donald, A. M. (1998). Chiral side-chain liquid-crystalline polymeric properties of starch. *Macromolecules, 31*(22), 7980–7984.

Zhang, G. Y., Ao, Z. H., & Hamaker, B. R. (2006). Slow digestion property of native cereal starches. *Biomacromolecules, 7*(11), 3252–3258.

Zhang, Y. H. P., Evans, B. R., Mielenz, J. R., Hopkins, R. C., & Adams, M. W. W. (2007). High-yield hydrogen production from starch and water by a synthetic enzymatic pathway. *PLoS ONE, 2*(5), e456.